Monthly Notices
of the
ROYAL ASTRONOMICAL SOCIETY

MNRAS **471,** 4966–4981 (2017)
Advance Access publication 2017 August 18

doi:10.1093/mnras/stx1544

The ASAS-SN bright supernova catalogue – III. 2016

T. W.-S. Holoien,[1,2★†] J. S. Brown,[1] K. Z. Stanek,[1,2★] C. S. Kochanek,[1,2★] B. J. Shappee,[3‡] J. L. Prieto,[4,5] Subo Dong,[6] J. Brimacombe,[7] D. W. Bishop,[8] S. Bose,[6] J. F. Beacom,[1,2,9] D. Bersier,[10] Ping Chen,[6] L. Chomiuk,[11] E. Falco,[12] D. Godoy-Rivera,[1] N. Morrell,[13] G. Pojmanski,[14] J. V. Shields,[1] J. Strader,[11] M. D. Stritzinger,[15] Todd A. Thompson,[1,2] P. R. Woźniak,[16] G. Bock,[17] P. Cacella,[18] E. Conseil,[19] I. Cruz,[20] J. M. Fernandez,[21] S. Kiyota,[22] R. A. Koff,[23] G. Krannich,[24] P. Marples,[25] G. Masi,[26] L. A. G. Monard,[27] B. Nicholls,[28] J. Nicolas,[29] R. S. Post,[30] G. Stone[31] and W. S. Wiethoff[32]

Affiliations are listed at the end of the paper

Accepted 2017 June 16. Received 2017 June 15; in original form 2017 May 11

ABSTRACT

This catalogue summarizes information for all supernovae discovered by the All-Sky Automated Survey for SuperNovae (ASAS-SN) and all other bright ($m_{\rm peak} \leq 17$), spectroscopically confirmed supernovae discovered in 2016. We then gather the near-infrared through ultraviolet magnitudes of all host galaxies and the offsets of the supernovae from the centres of their hosts from public data bases. We illustrate the results using a sample that now totals 668 supernovae discovered since 2014 May 1, including the supernovae from our previous catalogues, with type distributions closely matching those of the ideal magnitude limited sample from Li et al. This is the third of a series of yearly papers on bright supernovae and their hosts from the ASAS-SN team.

Key words: catalogues – surveys – supernovae: general.

1 INTRODUCTION

The last two decades have seen the proliferation of large, systematic surveys that search some or all of the sky for supernovae (SNe) and other transient phenomena. Significant examples include the Lick Observatory Supernova Search (LOSS; Li et al. 2000), the Panoramic Survey Telescope and Rapid Response System (Pan-STARRS; Kaiser et al. 2002), the Texas Supernova Search (Quimby 2006), the Sloan Digital Sky Survey (SDSS) Supernova Survey (Frieman et al. 2008), the Catalina Real-Time Transient Survey (CRTS; Drake et al. 2009), the CHilean Automatic Supernova sEarch (Pignata et al. 2009), the Palomar Transient Factory (Law et al. 2009), the *Gaia* transient survey (Hodgkin et al. 2013), the La Silla-QUEST Low Redshift Supernova Survey (Baltay et al. 2013), the Mobile Astronomical System of TElescope Robots (MASTER; Gorbovskoy et al. 2013) survey, the Optical Gravitational Lensing Experiment-IV (Wyrzykowski et al. 2014) and the Asteroid Terrestrial-impact Last Alert System (ATLAS; Tonry 2011).

Despite the number of transient survey projects, there has been no rapid-cadence optical survey scanning the entire visible sky to find the bright and nearby transients that can be observed in the greatest detail. Such events can provide the detailed observational data needed to have the greatest physical impact.

This is the goal of the All-Sky Automated Survey for SuperNovae (ASAS-SN;[1] Shappee et al. 2014). ASAS-SN is a long-term project designed to find bright transients, and has been highly successful since the beginning of survey operations, finding many interesting and nearby SNe (e.g. Dong et al. 2016a; Holoien et al. 2016a; Shappee et al. 2016a; Godoy-Rivera et al. 2017), tidal disruption events (Holoien et al. 2014a; Brown et al. 2016a, 2017; Holoien et al. 2016b,c; Prieto et al. 2016a; Romero-Cañizales et al. 2016), active galactic nucleus flares (Shappee et al. 2014), stellar outbursts (Holoien et al. 2014b; Schmidt et al. 2014, 2016; Herczeg et al. 2016) and cataclysmic variable stars (Kato et al. 2014a,b, 2015, 2016).

During 2016, ASAS-SN comprised eight 14-cm telescopes with standard *V*-band filters, each with a 4.5 × 4.5 deg field of view and a limiting magnitude of $m_V \sim 17$ [see Shappee et al. (2014) for further technical details]. These telescopes are divided into two

★ E-mail: tholoien@astronomy.ohio-state.edu (TW-SH); kstanek@astronomy.ohio-state.edu (KZS); ckochanek@astronomy.ohio-state.edu (CSK)
† US Department of Energy Computational Science Graduate Fellow.
‡ Hubble, Carnegie-Princeton Fellow.

[1] http://www.astronomy.ohio-state.edu/~assassin/

units, each with four telescopes on a common mount hosted by the Las Cumbres Observatory (Brown et al. 2013). Brutus, our northern unit, is housed at the Las Cumbres Observatory site on Mount Haleakala in Hawaii, and Cassius, our southern unit, is hosted at the Las Cumbres Observatory site at Cerro Tololo, Chile. The two units combined give ASAS-SN roughly 20 000 deg^2 of coverage per clear night, allowing us to cover the entire observable sky (roughly 30 000 deg^2 at any given time) with a 2–3 d cadence. In 2017, ASAS-SN will expand to five units (20 telescopes) at four sites (Hawaii, McDonald Observatory in Texas, Sutherland, South Africa, and two in Chile), allowing nightly coverage of the visible sky with little sensitivity to local weather. For a more detailed history of the ASAS-SN project, see the introduction of Holoien et al. (2017b) and Shappee et al. (2014).

ASAS-SN data are processed and searched in real time and all ASAS-SN discoveries are announced publicly upon confirmation, allowing for rapid discovery and response by both the ASAS-SN team and others. Our untargeted survey approach and complete spectroscopic identification make our sample less biased than those of many other SN searches. This makes it ideal for population studies of nearby SNe and their hosts.

This manuscript is the third of a series of yearly catalogues provided by the ASAS-SN team and presents collected information on SNe discovered by ASAS-SN in 2016 and their host galaxies. As in our previous catalogues (Holoien et al. 2017a,b), we also provide the same information for bright SNe (those with $m_{\rm peak} \leq 17$) that were discovered by other professional surveys and amateur astronomers in 2016 to construct a complete sample of bright SNe discovered in 2016. This includes whether ASAS-SN independently found the SNe after the initial announcement.

The analyses and information presented in this paper supersede the information presented in discovery and classification Astronomer's Telegrams (ATels), which we cite in this manuscript, and the information publicly available on ASAS-SN webpages and the Transient Name Server (TNS[2]).

In Section 2, we describe the sources of the information presented in this manuscript and list ASAS-SN supernovae with updated classifications or redshift measurements. In Section 3, we give statistics on the SN and host galaxy populations in our full cumulative sample, including the discoveries listed in Holoien et al. (2017a,b), and discuss overall trends in the sample. Throughout our analyses, we assume a standard ΛCDM cosmology with $H_0 = 69.3$ km s^{-1} Mpc^{-1}, $\Omega_{\rm M} = 0.29$ and $\Omega_\Lambda = 0.71$ for converting host redshifts into distances. In Section 4, we conclude with our overall findings and discuss how the upcoming expansion to ASAS-SN will impact our future discoveries.

2 DATA SAMPLES

Below we outline the sources of the data collected in our SN and host galaxy samples. These data are presented in Tables 1, 2, 3 and 4.

2.1 The ASAS-SN supernova sample

Table 1 includes information for all SNe discovered by ASAS-SN between 2016 January 1 and 2016 December 31. As in Holoien et al. (2017a,b), all names, discovery dates and host names are taken from our discovery ATels, all of which are cited in Table 1. We also include the SN names designated by TNS, the official International Astronomical Union (IAU) mechanism for reporting new astronomical transients. As is noted in our ATels, the ASAS-SN team is participating in the TNS system to minimize potential confusion, but we use the ASAS-SN designations as our primary nomenclature and encourage others to do the same in order to preserve the origin of the transient in future literature.

ASAS-SN supernova redshifts were spectroscopically measured from classification spectra. For those cases where an SN host had a previously measured redshift and the host redshift is consistent with the transient redshift, we list the redshift of the host taken from the NASA/IPAC Extragalactic Database (NED).[3] For all other cases, we typically report the redshifts given in the classification telegrams, excepting those that have been updated in this work (see below).

ASAS-SN supernova classifications are taken from classification telegrams, which we have cited in Table 1, when available. In some cases, a classification was only reported on TNS and was not reported in an ATel; for these cases, we list 'TNS' in the 'Classification Telegram' column. When available in the classification ATel or on TNS, we also give the approximate age at discovery measured in days relative to peak. Classifications were typically obtained using either the Supernova Identification code (SNID; Blondin & Tonry 2007) or the Generic Classification Tool (GELATO;[4] Harutyunyan et al. 2008), which both compare observed input spectra to template spectra in order to estimate the SN age and type.

Using archival classification and late-time spectra of the ASAS-SN supernova discoveries taken from TNS and Weizmann Interactive Supernova data REPository (WISEREP; Yaron & Gal-Yam 2012), we also update a number of redshifts and classifications that differ from what was reported in the discovery and classification telegrams. ASASSN-16ah, ASASSN-16bm, ASASSN-16bq, ASASSN-16bv, ASASSN-16cr, ASASSN-16cs, ASASSN-16es, ASASSN-16fa, ASASSN-16fc, ASASSN-16fx, ASASSN-16gz, ASASSN-16hr, ASASSN-16hw, ASASSM-16ip, ASASSN-16je, ASASSN-16jj, ASASSN-16la, ASASSN-16lc, ASASSN-16ll, ASASSN-16mj, ASASSN-16ns, ASASSN-16oj, ASASSN-16ok, ASASSN-16ol, ASASSN-16oy, ASASSN-16pd, ASASSN-16pj and ASASSN-16pk have updated redshifts based on archival spectra. ASASSN-16dx has been reclassified from archival spectra, and ASASSN-16fp has been classified as a Ib/Ic-BL (Yamanaka et al. 2017). All updated redshifts and classifications are reported in Table 1.

Using the ASTROMETRY.NET (Barron et al. 2008; Lang et al. 2010) package, we solved the astrometry in follow-up images for all ASAS-SN supernovae and measured a centroid position for the SN using IRAF. This approach typically yields errors of $<$1.0 arcsec in position, which is significantly more accurate than measuring the SN position directly in ASAS-SN images, which have a 7.0 arcsec pixel scale. The images used to measure astrometry were obtained using the Las Cumbres Observatory 1-m telescopes (Brown et al. 2013), the Ohio State Multi-Object Spectrograph (OSMOS) mounted on the MDM Hiltner 2.4-m telescope, or from amateur collaborators working with the ASAS-SN team. For most cases, the coordinates measured from follow-up images were reported in our discovery ATels, but we report new, more accurate coordinates in Table 1 for those cases where the SNe were announced with coordinates measured in ASAS-SN data. The offset from the host galaxy

[2] https://wis-tns.weizmann.ac.il/

[3] https://ned.ipac.caltech.edu/

[4] gelato.tng.iac.es

Table 1. ASAS-SN Supernovae. This table is available in its entirety in a machine-readable form in the online journal. A portion is shown here for guidance regarding its form and content.

SN Name	IAU name	Discovery date	RA[a]	Dec.[a]	Redshift	V_{disc}[b]	V_{peak}[b]	Offset (arcsec)[c]	Type	Age at disc[d]	Host name	Discovery ATel	Classification ATel
ASASSN-16aa	2016A	2016-01-02.42	08:09:14.55	+00:16:50.6	0.017 38	16.8	16.4	7.99	Ia	−4	UGC 04251	Brown et al. (2016b)	Pan et al. (2016a)
ASASSN-16ab	2016B	2016-01-03.62	11:55:04.20	+01:43:07.2	0.004 29	14.7	14.7	11.36	II	−4	CGCG 012−116	Shappee et al. (2016b)	Piascik & Steele (2016a)
ASASSN-16ad	2016F	2016-01-09.28	01:39:32.05	+33:49:36.3	0.016 14	16.2	15.1	13.99	Ia	–	KUG 0136+335	Dong et al. (2016b)	Rui et al. (2016a)
ASASSN-16ah	2016J	2016-01-11.34	05:47:45.38	+53:36:32.3	0.028 50	16.8	16.7	9.19	Ia	−8	Uncatalogued	Brimacombe et al. (2016a)	Brimacombe et al. (2016a)
ASASSN-16ai	2016I	2016-01-12.58	14:39:44.77	+23:23:42.5	0.014 90	17.0	16.7	8.99	IIP	–	UGC 09450	Brown et al. (2016c)	Xin & Zhang (2016)
ASASSN-16aj	2016K	2016-01-14.21	04:21:48.21	−15:45:19.3	0.030 75	17.0	14.1	8.95	Ia	−2	NGC 1562	Brimacombe et al. (2016b)	Zhang (2016)
ASASSN-16al	2016L	2016-01-15.36	15:00:27.47	−13:33:09.0	0.009 30	17.0	16.5	49.94	IIP	–	UGCA 397	Kiyota et al. (2016a)	Dimitriadis et al. (2016)
ASASSN-16am	2016N	2016-01-15.36	04:45:21.28	+73:23:41.1	0.015 02	17.4	17.1	14.33	II	2	CGCG 328−018	Masi et al. (2016a)	Piascik & Steele (2016b)
ASASSN-16ar	2016Z	2016-01-17.21	04:28:30.83	−17:39:23.4	0.031 08	17.0	16.5	0.14	Ia	1	2MASX J04283087−1739233	Masi et al. (2016b)	Masi et al. (2016b)
ASASSN-16at	2016X	2016-01-20.59	12:55:15.50	+00:05:59.7	0.004 41	15.1	14.0	73.00	II	–	UGC 08041	Bock et al. (2016a)	Hosseinzadeh et al. (2016a)
ASASSN-16av	2016ac	2016-01-18.44	11:51:28.24	+22:01:33.7	0.025 67	16.5	16.0	0.26	Ia	−7	NGC 3926 NED02	Holoien et al. (2016d)	Holoien et al. (2016d)
ASASSN-16aw	2016yr	2016-01-29.27	05:39:57.45	−40:30:57.9	0.037 28	17.0	16.3	61.53	Ia	−1	ESO 306−G 016	Kiyota et al. (2016b)	Cikota et al. (2016a)
ASASSN-16ax	2016ag	2016-01-26.23	01:31:23.18	+60:19:13.7	0.018 70	16.0	15.7	2.24	Ia	−5	2MASX J01312331+6019128	Masi et al. (2016c)	Falco et al. (2016a)
ASASSN-16ay	2016ys	2016-01-28.41	07:12:14.35	+07:14:23.2	0.028 34	16.7	16.3	14.02	Ia	−2	UGC 03738	Koff et al. (2016a)	Cikota et al. (2016a)
ASASSN-16az	2016za	2016-01-29.38	11:30:33.73	−42:33:31.4	0.034 07	16.9	16.4	4.69	Ia	9	2MASX J11303364−4233359	Holoien et al. (2016e)	Prieto, Rich & Shappee (2016b)
ASASSN-16ba	2016zb	2016-01-29.34	09:42:29.22	−16:58:26.9	0.013 92	16.8	14.9	10.06	II	5	MCG -03-25-015	Holoien et al. (2016e)	Hosseinzadeh et al. (2016b)
ASASSN-16bb	2016zc	2016-01-31.60	14:05:57.10	+43:53:02.2	0.033 75	16.6	16.2	5.78	Ia-91T	−7	SDSS J140557.36+435257.2	Kiyota et al. (2016c)	Piascik & Steele (2016c)
ASASSN-16bc	2016zd	2016-02-02.28	12:05:25.83	−21:24:01.2	0.031 94	17.0	16.4	14.48	Ia	−10	2MASX J12052488−2123572	Fernandez et al. (2016a)	Piascik & Steele (2016c)
ASASSN-16bg	2016acx	2016-02-06.47	12:59:25.10	+27:44:25.0	0.020 22	17.4	16.8	5.68	Ia	14	2MASX J12592491+2744198	Brown et al. (2016d)	Faran et al. (2016)
ASASSN-16bl	2016adk	2016-02-08.22	11:42:26.68	−36:54:23.4	0.029 55	17.3	16.8	2.28	Ia	0	2MASX J11422674-3654256	Brimacombe et al. (2016c)	Terreran et al. (2016a)

Notes. [a]Right ascension and declination are given in the J2000 epoch.
[b]All magnitudes are *V*-band magnitudes from ASAS-SN.
[c]Offset indicates the offset of the SN in arcseconds from the coordinates of the host nucleus, taken from NED.
[d]Discovery ages are given in days relative to peak. All ages are approximate and are only listed if a clear age was given in the classification telegram.

Table 2. Non-ASAS-SN Supernovae. This table is available in its entirety in a machine-readable form in the online journal. A portion is shown here for guidance regarding its form and content.

SN name	IAU name[a]	Discovery date	RA[b]	Dec.[b]	Redshift	m_{peak}[c]	Offset (arcsec)[d]	Type	Host name	Discovered by[e]	Recovered?[f]
2016D	2016D	2016-01-01.55	04:01:25.99	−54:45:30.8	0.045 10	16.5	2.23	Ia	2MASX J04012613−5445295	Amateurs	Yes
2016C	2016C	2016-01-03.84	13:38:05.30	−17:51:15.3	0.004 52	14.9	112.25	IIP	NGC 5247	Amateurs	Yes
MASTER OT J165420.77-615258	–	2016-01-06.00	16:54:20.77	−61:52:58.0	0.015 05	16.9	8.04	IIP	ESO 138−G006	MASTER	No
2016G	2016G	2016-01-09.94	03:03:57.74	+43:24:03.5	0.009 15	16.3	16.68	Ic-BL	NGC 1171	Amateurs	Yes
2016P	2016P	2016-01-19.19	13:57:31.10	+06:05:51.0	0.014 62	16.0	21.88	Ic-BL	NGC 5374	Amateurs	Yes
2016W	2016W	2016-01-20.49	02:30:39.69	+42:14:08.9	0.019 25	16.0	18.44	Ia	NGC 946	Amateurs	Yes
ATLAS16aaf	2016ado	2016-01-20.78	02:03:05.79	−03:50:28.0	0.042 48	17.0	3.18	Ia-07if	2MASX J02030578−0350240	ATLAS	No
ATLAS16aab	2016adp	2016-01-21.81	03:21:42.43	+42:05:49.4	0.018 00	16.5	6.36	Ia-91bg	2MASX J03214217+4205549	ATLAS	No
MASTER OT J105908.57+103834.8	–	2016-01-31.06	10:59:08.57	+10:38:34.8	0.035 00	16.8	5.16	Ia	SDSS J105908.63+103829.7	MASTER	Yes
2016adi	2016adi	2016-02-03.54	13:47:43.11	−30:55:57.0	0.014 90	15.3	46.56	Ia	NGC 5292	Amateurs	No
2016adj	2016adj	2016-02-08.56	13:25:24.12	−43:00:57.9	0.001 83	14.3	39.56	IIb	NGC 5128	Amateurs	No
2016afa	2016afa	2016-02-12.92	15:36:32.47	+16:36:36.7	0.006 53	16.8	12.45	II	NGC 5962	Amateurs	Yes
2016ajf	2016ajf	2016-02-18.44	03:19:54.47	+41:33:53.5	0.020 31	16.9	6.42	Ia	NGC 1278	Amateurs	Yes
Gaia16aeu	2016ajm	2016-02-20.09	02:49:36.01	−31:13:23.9	0.021 36	16.9	14.70	Ia-91bg	2dFGRS S394Z183	*Gaia*	No
Gaia16agf	2016aqs	2016-02-27.28	06:34:08.98	−25:11:04.6	0.030 00	17.0	20.09	Ia	Uncatalogued	*Gaia*	Yes
2016aqt	2016aqt	2016-12-28.44	13:45:50.75	+26:47:47.4	0.050 46	16.5	2.16	Ia-91T	SDSS J134550.90+264747.4	Amateurs	Yes
PS16bdu	2016bdu	2016-02.28.62	13:10:13.95	+32:31:14.1	0.017 00	16.5	2.16	IIn	SDSS J131014.04+323115.9	Pan-STARRS	Yes
2016bam	2016bam	2016-03-07.43	07:46:52.72	+39:01:21.8	0.013 50	15.8	33.80	II	NGC 2444	Amateurs	Yes
ATLAS16ago	2016bev	2016-03-10.33	07:47:50.21	−18:44:12.8	0.010 80	16.7	50.82	IIP	ESO 560−G013	ATLAS	No
2016bas	2016bas	2016-03-12.51	07:38:05.53	−55:11:47.0	0.009 41	16.8	20.02	IIb	ESO 163−G011	Amateurs	No

Notes. [a]IAU name is not provided if one was not given to the SN. In some cases the IAU name may also be the primary SN name.
[b]Right ascension and declination are given in the J2000 epoch.
[c]All magnitudes are taken from D. W. Bishop's Bright Supernova website, as described in the text, and may be from different filters.
[d]Offset indicates the offset of the SN in arcseconds from the coordinates of the host nucleus, taken from NED.
[e]'Amateurs' indicates discovery by any number of non-professional astronomers, as described in the text.
[f]Indicates whether the SN was independently recovered in ASAS-SN data or not.

Table 3. ASAS-SN supernova host galaxies. This table is available in its entirety in a machine-readable form in the online journal. A portion is shown here for guidance regarding its form and content. Uncertainty is given for all magnitudes, and in some cases is equal to zero.

Galaxy name	Redshift	SN name	SN type	SN offset (arcsec)	A_V[a]	m_{NUV}[b]	m_u[c]	m_g[c]	m_r[c]	m_i[c]	m_z[c]	m_J[d]	m_H[d]	m_{K_S}[d,e]	m_{W1}	m_{W2}
UGC 04251	0.017 38	ASASSN-16aa	Ia	7.99	0.124	–	18.37 0.02	16.41 0.00	15.59 0.00	15.11 0.00	14.73 0.00	11.55 0.03	10.85 0.03	10.57 0.05	10.81 0.02	10.75 0.02
PGC 037392	0.004 29	ASASSN-16ab	II	11.36	0.058	16.56 0.02	16.05 0.01	15.21 0.00	14.92 0.00	14.78 0.00	14.67 0.01	13.91 0.09	13.34 0.10	13.02 0.16	13.69 0.03	13.57 0.04
KUG 0136+335	0.016 14	ASASSN-16ad	Ia	13.99	0.134	17.82 0.03	16.93 0.05	15.83 0.01	15.38 0.01	15.14 0.02	14.98 0.08	15.20 0.08	14.49 0.11	14.54 0.20	14.21 0.03	14.03 0.04
Uncatalogued	0.028 50	ASASSN-16ah	Ia	9.19	0.719	20.34 0.25	–	–	–	–	–	>16.5	>15.7	14.09 0.06*	14.63 0.04	14.39 0.06
UGC 09450	0.014 90	ASASSN-16ai	IIP	8.99	0.088	17.61 0.06	17.31 0.02	16.38 0.01	16.08 0.01	15.87 0.01	16.06 0.03	16.09 0.10	15.66 0.15	15.78 0.19	15.62 0.04	15.29 0.08
NGC 1562	0.030 75	ASASSN-16aj	Ia	8.95	0.090	20.02 0.17	–	–	–	–	–	12.08 0.03	11.37 0.04	11.08 0.06	11.37 0.02	11.44 0.02
UGCA 397	0.009 30	ASASSN-16al	IIP	49.94	0.276	16.89 0.04	–	–	–	–	–	>16.5	>15.7	14.44 0.06*	14.98 0.04	14.86 0.09
CGCG 328−018	0.015 02	ASASSN-16am	II	14.33	0.470	20.49 0.18	–	–	–	–	–	11.63 0.03	10.91 0.04	10.67 0.05	11.21 0.02	11.28 0.02
2MASX J04283087−1739233	0.031 08	ASASSN-16ar	Ia	0.14	0.105	–	–	–	–	–	–	12.62 0.03	11.97 0.05	11.66 0.07	11.89 0.02	11.93 0.02
UGC 08041	0.004 41	ASASSN-16at	II	73.00	0.061	14.57 0.01	15.72 0.01	14.10 0.00	13.48 0.00	13.23 0.00	13.25 0.01	12.92 0.05	12.32 0.07	12.04 0.11	13.01 0.03	13.03 0.03
NGC 3926 NED02	0.025 67	ASASSN-16av	Ia	0.26	0.075	19.11 0.09	16.12 0.01	14.27 0.00	13.38 0.00	12.99 0.00	12.67 0.00	11.65 0.02	10.97 0.03	10.65 0.03	11.13 0.02	11.22 0.02
ESO 306−G 016	0.037 28	ASASSN-16aw	Ia	61.53	0.088	–	–	–	–	–	–	11.80 0.03	11.07 0.03	10.78 0.06	11.32 0.02	11.32 0.02
2MASX J01312331+6019128	0.018 70	ASASSN-16ax	Ia	2.24	1.512	–	–	–	–	–	–	12.47 0.03	11.65 0.03	11.36 0.05	11.44 0.02	11.46 0.02
UGC 03738	0.028 34	ASASSN-16ay	Ia	14.02	0.189	–	–	–	–	–	–	12.52 0.04	11.83 0.05	11.55 0.08	11.95 0.02	11.99 0.02
2MASX J11303364−4233359	0.034 07	ASASSN-16az	Ia	4.69	0.235	–	–	–	–	–	–	13.57 0.05	12.87 0.05	12.53 0.08	12.50 0.02	12.49 0.02
MCG -03-25-015	0.013 92	ASASSN-16ba	II	10.06	0.180	16.85 0.03	–	–	–	–	–	>16.5	>15.7	14.12 0.06*	14.66 0.03	14.58 0.06
SDSS J140557.36+435257.2	0.033 75	ASASSN-16bb	Ia-91T	5.78	0.020	18.89 0.08	18.31 0.04	17.29 0.01	16.96 0.01	16.76 0.01	16.71 0.08	>16.5	>15.7	15.06 0.06*	15.60 0.04	15.40 0.08
2MASX J12052488−2123572	0.031 94	ASASSN-16bc	Ia	14.48	0.152	18.26 0.06	–	–	–	–	–	12.78 0.04	12.11 0.04	11.76 0.07	11.99 0.02	11.58 0.02
2MASX J12592491+2744198	0.020 22	ASASSN-16bg	Ia	5.68	0.024	20.94 0.26	17.65 0.01	15.86 0.00	15.05 0.00	14.65 0.00	14.35 0.00	13.30 0.03	12.55 0.04	12.35 0.05	12.33 0.02	12.43 0.02
2MASX J11422674−3654256	0.029 55	ASASSN-16bl	Ia	2.28	0.318	–	–	–	–	–	–	12.72 0.04	11.92 0.04	11.63 0.07	11.81 0.02	11.83 0.02

Notes. [a]Galactic extinction taken from Schlafly & Finkbeiner (2011).
[b]No magnitude is listed for those galaxies not detected in *GALEX* survey data.
[c]No magnitude is listed for those galaxies not detected in SDSS data or those located outside of the SDSS footprint.
[d]For those galaxies not detected in 2MASS data, we assume an upper limit of the faintest galaxy detected in each band from our sample.
[e]K_S-band magnitudes marked with a '*' indicate those estimated from the *WISE* $W1$-band data, as described in the text.

Table 4. Non-ASAS-SN supernova host galaxies. This table is available in its entirety in a machine-readable form in the online journal. A portion is shown here for guidance regarding its form and content. Uncertainty is given for all magnitudes, and in some cases is equal to zero. 'MASTER' SN names have been abbreviated for space reasons.

Galaxy name	Redshift	SN name	SN type	SN offset (arcsec)	A_V[a]	m_{NUV}[b]	m_u[c]	m_g[c]	m_r[c]	m_i[c]	m_z[c]	m_J[d]	m_H[d]	m_{K_S}[d,e]	m_{W1}	m_{W2}
2MASX J04012613−5445295	0.045 10	2016D	Ia	2.23	0.035	19.96 0.18	–	–	–	–	–	12.34 0.03	11.63 0.04	11.26 0.06	11.49 0.02	11.55 0.02
NGC 5247	0.004 52	2016C	IIP	112.25	0.244	–	–	–	–	–	–	8.80 0.02	8.17 0.02	7.93 0.03	10.46 0.02	10.34 0.02
ESO 138−G006	0.015 05	MASTER J165420.77	IIP	8.04	0.425	–	–	–	–	–	–	>16.5	>15.7	13.57 0.07*	14.21 0.04	14.00 0.04
NGC 1171	0.009 15	2016G	Ic-BL	16.68	0.431	15.89 0.02	15.31 0.01	13.54 0.00	12.64 0.00	12.18 0.00	11.84 0.00	10.79 0.02	10.10 0.02	9.80 0.03	10.87 0.02	10.89 0.02
NGC 5374	0.014 62	2016P	Ic-BL	21.88	0.074	15.12 0.01	14.52 0.01	13.31 0.00	12.53 0.00	12.13 0.00	11.82 0.00	10.81 0.03	10.16 0.04	9.88 0.06	10.86 0.02	10.67 0.02
NGC 946	0.019 25	2016W	Ia	18.44	0.191	18.83 0.12	–	–	–	–	–	10.83 0.02	10.11 0.02	9.82 0.02	10.25 0.02	10.25 0.02
2MASX J02030578−0350240	0.042 48	ATLAS16aaf	Ia-07if	3.18	0.069	20.06 0.11	17.59 0.02	15.92 0.00	15.26 0.00	14.93 0.00	14.71 0.00	13.76 0.04	13.07 0.05	12.80 0.07	12.85 0.04	12.83 0.04
2MASX J03214217+4205549	0.018 00	ATLAS16aab	Ia-91bg	6.36	0.513	–	18.14 0.03	16.30 0.00	15.37 0.00	14.90 0.00	14.53 0.01	13.62 0.05	12.87 0.07	12.58 0.09	13.16 0.04	13.20 0.04
SDSS J105908.63+103829.7	0.035 00	MASTER J105908.57	Ia	5.16	0.069	21.29 0.22	21.31 0.32	20.18 0.05	19.77 0.06	19.57 0.06	19.93 0.32	>16.5	>15.7	16.92 0.22*	17.56 0.21	16.49 0.29
NGC 5292	0.014 90	2016adi	Ia	46.56	0.164	15.76 0.02	–	–	–	–	–	9.78 0.02	9.13 0.03	8.84 0.03	10.07 0.02	10.12 0.02
NGC 5128	0.001 83	2016adj	IIb	39.56	0.315	–	–	–	–	–	–	5.03 0.02	4.31 0.02	3.99 0.02	5.26 0.05	4.76 0.04
NGC 5962	0.006 53	2016afa	II	12.45	0.149	14.11 0.01	13.89 0.00	12.27 0.00	11.51 0.00	11.14 0.00	10.69 0.00	9.58 0.01	8.89 0.01	8.61 0.02	9.67 0.02	9.53 0.02
NGC 1278	0.020 31	2016ajf	Ia	6.42	0.451	19.11 0.05	–	–	–	–	–	10.30 0.02	9.57 0.02	9.25 0.03	10.10 0.02	10.14 0.02
2dFGRS S394Z183	0.021 36	Gaia16aeu	Ia-91bg	14.70	0.069	20.43 0.13	–	–	–	–	–	>16.5	>15.7	14.77 0.07*	15.41 0.04	15.80 0.11
Uncatalogued	0.030 00	Gaia16agf	Ia	20.09	0.182	–	–	–	–	–	–	>16.5	>15.7	>15.6	–	–
SDSS J134550.90+264747.4	0.050 46	2016aqt	Ia-91T	2.16	0.046	19.14 0.11	18.79 0.07	17.75 0.01	17.45 0.01	17.24 0.02	17.10 0.05	>16.5	>15.7	15.51 0.08*	16.15 0.05	16.09 0.15
SDSS J131014.04+323115.9	0.017 00	PS16bdu	IIn	2.16	0.041	–	22.08 0.28	21.19 0.06	20.94 0.07	20.99 0.11	21.07 0.39	>16.5	>15.7	>15.6	–	–
NGC 2444	0.013 50	2016bam	II	33.80	0.140	–	15.57 0.01	13.73 0.00	12.84 0.00	12.41 0.00	12.10 0.00	11.17 0.02	10.47 0.02	10.21 0.03	10.39 0.02	10.48 0.02
ESO 560−G013	0.010 80	ATLAS16ago	IIP	50.82	1.050	–	–	–	–	–	–	10.09 0.02	9.26 0.02	8.90 0.02	10.45 0.02	10.27 0.02
ESO 163−G011	0.009 41	2016bas	IIb	20.02	0.407	–	–	–	–	–	–	10.81 0.02	10.01 0.02	9.64 0.03	10.32 0.02	10.08 0.02

Notes. [a]Galactic extinction taken from Schlafly & Finkbeiner (2011).
[b]No magnitude is listed for those galaxies not detected in *GALEX* survey data.
[c]No magnitude is listed for those galaxies not detected in SDSS data or those located outside of the SDSS footprint.
[d]For those galaxies not detected in 2MASS data, we assume an upper limit of the faintest galaxy detected in each band from our sample.
[e]K_S-band magnitudes marked with a '*' indicate those estimated from the *WISE* $W1$-band data, as described in the text.

nucleus is also reported, and was calculated using the coordinates measured from follow-up images and host coordinates available in NED.

V-band, host-subtracted discovery and peak magnitudes were re-measured from ASAS-SN data for all ASAS-SN supernova discoveries, and these magnitudes are reported in Table 1. This has resulted in differences between the magnitudes reported in this work and the magnitudes reported in the original discovery ATels for some cases, where re-reduction of the data has led to improvements in our photometry. We define the 'discovery magnitude' as the magnitude of the SN on the announced discovery date. For cases with enough detections in the light curve, we also perform a parabolic fit to the light curve and estimate a peak magnitude based on the fit. The 'peak magnitude' reported in Table 1 is the brighter value between the brightest measured magnitude and the peak of the parabolic fit.

We include all SNe discovered by ASAS-SN in 2016 in this catalogue and in Table 1, including those that peaked at magnitudes fainter than $m_V = 17$. In the comparison analyses presented in Section 3, however, we include only those ASAS-SN supernovae with $m_{V,\mathrm{peak}} \leq 17$ so that our sample is consistent with the non-ASAS-SN sample.

2.2 The non-ASAS-SN supernova sample

In Table 2, we give information for all spectroscopically confirmed SNe with peak magnitudes of $m_{\mathrm{peak}} \leq 17$ that were discovered by other professional and amateur SN searches between 2016 January 1 and 2016 December 31.

We compiled data for the non-ASAS-SN discoveries from the 'latest supernovae' website[5] designed and maintained by D. W. Bishop (Gal-Yam et al. 2013). This site compiles discoveries reported from different channels and links objects reported by different sources at different times, making it an ideal source for collecting information on SNe discovered by different search groups. While we did use TNS for verification of the data from the latest SNe website, we did not use it as the primary source of information on non-ASAS-SN discoveries, as some SN searches do not participate in the TNS system.

Names, IAU names, discovery dates, coordinates, host names, host offsets, peak magnitudes, spectral types and discovery sources for each SN in the non-ASAS-SN sample were taken from the latest SNe website when possible. Host galaxy redshifts were collected from NED when available and were taken from the latest SNe website otherwise. For cases where a host name or host offset was not listed on the website for an SN, the primary name and offset were taken from NED. In these cases, we define the offset as the distance between the reported coordinates of the SN and the galaxy coordinates in NED. In some cases, no catalogued galaxy was listed at the position of the host in NED, but a host galaxy was clearly visible in archival Pan-STARRS data (Chambers et al. 2016). In these cases, we measured the centroid position of the host nucleus using IRAF and calculated the offset using those coordinates. For all SNe in both samples, we use the primary name of the host galaxy listed in NED, which sometimes differs from the name listed on the ASAS-SN supernova page or the latest SN website.

We update the redshifts and classifications of several SNe discovered by non-ASAS-SN sources that have missing or incorrect information on the latest SNe website. Using archival classification and late-time spectra from TNS and WISeREP, we have updated the classifications of SN 2016ajf, SN 2016bau, SN 2016gxp, KAIT-16az, Gaia16cbd and SN 2016aqt, which were previously mis-typed. CSS160708:151956+052419/SN 2016ehy has a redshift of $z = 0.045$ (Shivvers, private communication) and Gaia16alq/SN 2016dxv has a redshift of $z = 0.023$ (Piascik, private communication), measured from SN lines in the spectra in both cases. Finally, based on an examination of available spectra, PS16dtm/SN 2016ezh, which was previously reported as a Type-II superluminous supernova (SLSN-II; Dong et al. 2016d; Terreran et al. 2016b), appears to be a highly unique object, possibly consistent with an SLSN-II, a tidal disruption event, or even rare active galactic nucleus activity (e.g. Blanchard et al. 2017). For this reason, we include it in the catalogue, but exclude it from the analyses that follow. All updated types and redshifts are reported in Table 2.

The name of the discovery group is listed for all SNe discovered by other professional surveys. For those SNe discovered by non-professional astronomers, we list 'Amateurs' as the discovery source to differentiate these from those discovered by ASAS-SN and other professional astronomers and surveys. As in previous years, amateurs account for the largest number of bright SN discoveries in 2016 after ASAS-SN.

As in our previous catalogues, we note in Table 2 if the ASAS-SN team independently recovered these SNe while scanning our data. This is done to help quantify the impact ASAS-SN has on the discovery of bright SNe in the absence of other SNe searches.

2.3 The host galaxy samples

For the host galaxies of both SN samples, we collected Galactic extinction estimates for the direction to the host and host magnitudes spanning from the near-ultraviolet (NUV) to the infrared (IR) wavelengths. We present these data in Tables 3 and 4 for ASAS-SN hosts and non-ASAS-SN hosts, respectively. Galactic A_V from Schlafly & Finkbeiner (2011) at the positions of the SNe were gathered from NED. NUV magnitudes are taken from the *Galaxy Evolution Explorer* (*GALEX*; Morrissey et al. 2007) All Sky Imaging Survey, optical *ugriz* magnitudes are gathered from the Sloan Digital Sky Survey Data Release 13 (SDSS DR13; Albareti et al. 2016), NIR JHK_S magnitudes are gathered from the Two-Micron All Sky Survey (2MASS; Skrutskie et al. 2006) and IR *W*1 and *W*2 magnitudes are gathered from the *Wide-field Infrared Survey Explorer* (*WISE*; Wright et al. 2010) AllWISE source catalogue.

When a host galaxy was not detected in 2MASS, we adopted an upper limit corresponding to the faintest 2MASS host magnitudes in our sample for the *J* and *H* bands ($m_J > 16.5$, $m_H > 15.7$). For hosts that are not detected in 2MASS but are detected in the *WISE* *W*1 band, we estimated a host magnitude by adding the mean K_S–*W*1 offset from the sample to the *WISE* *W*1 data. This offset was calculated by averaging the offsets for all hosts that are detected in both the K_S and *W*1 bands from both SN samples from 2014 May 1 through 2016 December 31. The average offset is equal to −0.51 mag with a scatter of 0.04 mag and a standard error of 0.002 mag. If a host was not detected in either 2MASS or *WISE*, we adopted an upper limit of $m_{K_S} > 15.6$, corresponding to the faintest detected host in our sample.

3 ANALYSIS OF THE SAMPLE

Combining all the bright SNe discovered between 2014 May 1, when ASAS-SN became operational in both hemispheres, and 2016 December 31 provides a sample of 668 SNe once we exclude ASAS-SN discoveries with $m_{\mathrm{peak}} > 17.0$ (Holoien et al. 2017a,b). Of these,

[5] http://www.rochesterastronomy.org/snimages/

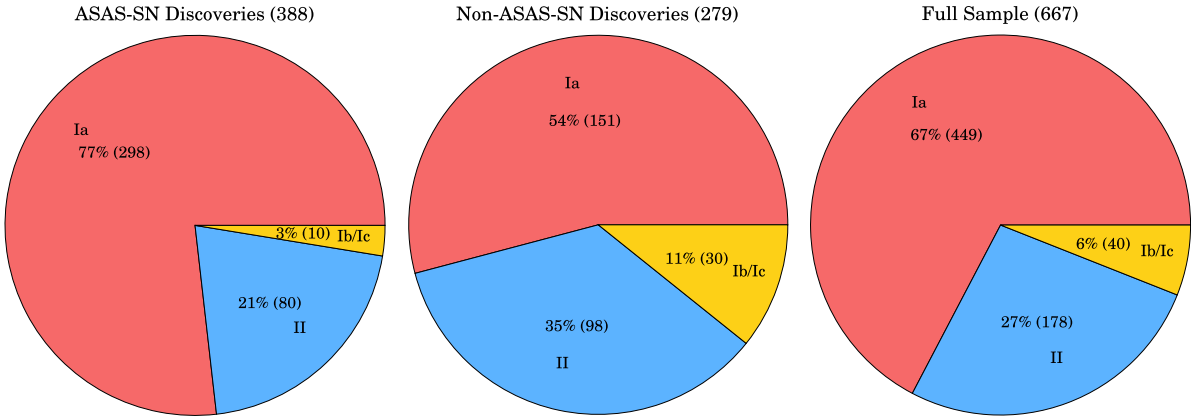

Figure 1. Left-hand panel: breakdown by type of the SNe discovered by ASAS-SN between 2014 May 1 and 2016 December 31. The proportions of each type are very similar to that of an ideal magnitude-limited sample (Li et al. 2011). Centre panel: the same chart for the non-ASAS-SN sample in the same time period. Right-hand panel: the same breakdown of types for the combined SN sample. For the purposes of this analysis, we exclude superluminous SNe and include Type IIb SNe in the 'Type II' sample.

58 per cent (389) were discovered by ASAS-SN, 21 per cent (137) were discovered by other professional surveys and 21 per cent (142) were discovered by amateur astronomers. 449 were Type Ia SNe, 178 were Type II SNe, 40 were Type Ib/Ic SNe and 1 was a superluminous SN. As in our previous catalogues, we consider Type IIb SNe as part of the Type II sample to allow for more direct comparison with the results of Li et al. (2011). ASASSN-15lh is excluded in analyses that follow looking at trends by type, as all available evidence points to it being an extremely luminous Type I SLSN (Dong et al. 2016a; Godoy-Rivera et al. 2017), though it has also been classified as a tidal disruption event around a Kerr black hole (Leloudas et al. 2016). ASAS-SN discoveries account for 66 per cent of the Type Ia SNe, 45 per cent of the Type II SNe and 25 per cent of the Type Ib/Ic SNe. Amateur discoveries account for 16, 30 and 48 per cent of the Type Ia, Type II and Type Ib/Ic SNe in the sample, respectively, and discoveries from other professional surveys account for the remaining 18, 25 and 28 per cent of each type.

Fig. 1 shows pie charts breaking down the type distributions of SNe in the ASAS-SN, non-ASAS-SN and combined samples. Type Ia SNe represent the largest fraction of SNe in all three samples, as expected for a magnitude-limited sample (e.g. Li et al. 2011). Comparing to the 'ideal magnitude-limited sample' breakdown predicted from the LOSS sample in Li et al. (2011), where there are 79 per cent Type Ia, 17 per cent Type II and 4 per cent Type Ib/Ic, the ASAS-SN sample matches the LOSS prediction almost exactly. The non-ASAS-SN sample and the combined sample have higher fractions of core-collapse SNe, as was the case in our previous catalogues (Holoien et al. 2017a,b).

ASAS-SN continues to be the dominant source of bright SN discoveries, and we often discover SNe shortly after explosion due to our rapid cadence: of the 336 ASAS-SN discoveries with approximate discovery ages, 69 per cent (232) were discovered prior to reaching their peak brightness. As was seen in Holoien et al. (2017a), ASAS-SN is less affected by host galaxy selection effects than other bright SN searches. For example, 25 per cent (96) of the ASAS-SN bright SNe were found in catalogued hosts that did not have previous redshift measurements available in NED, and an additional 4 per cent (14) were discovered in uncatalogued hosts or have no apparent host galaxy. Conversely, only 16 per cent (44) of non-ASAS-SN discoveries were found in catalogued hosts without redshift measurements, and only 3 per cent (8) were in uncatalogued galaxies or were hostless.

As we showed in our previous catalogues, ASAS-SN discoveries have a smaller average offset from their host galaxy nuclei than bright SNe discovered by other searches. The host galaxy K_S-band absolute magnitudes and the offsets of the SNe from the host centres for all SNe in our sample are shown in Fig. 2. The median offsets and magnitudes are shown with horizontal and vertical lines for each SN source (ASAS-SN, amateurs or other professionals). A luminosity scale corresponding to the magnitude scale is given on the upper axis of the figure to help put the magnitude scale in perspective, assuming that a typical $L_\star$ galaxy has $M_{\star,K_S} = -24.2$ (Kochanek et al. 2001).

Amateur SN searches tend to observe bright, nearby galaxies and use less sophisticated detection techniques than professional surveys, resulting in discoveries that are significantly biased towards more luminous hosts and larger offsets from the host nucleus. As we found previously (Holoien et al. 2017a), other professional surveys continue to discover SNe with smaller angular separations than amateurs (median value of 11.8 arcsec versus 16.5 arcsec), but show a similar median offset in terms of physical separation (5.0 kpc for professionals, 5.2 kpc for amateurs). ASAS-SN continues to be less biased against discoveries close to the host nucleus than either comparison group, as ASAS-SN discoveries show median offsets of 5.0 arcsec and 2.6 kpc.

These trends are more easily visible when looking at the cumulative distributions of the host galaxy magnitudes and offsets from host nuclei, as shown in Fig. 3. The distributions clearly show that the ASAS-SN and other professional samples stand out from the amateur sample in host galaxy luminosity, and that SNe discovered by ASAS-SN are more concentrated towards the centres of their hosts than those discovered by either amateurs or other professionals. While the majority of non-ASAS-SN professional discoveries continue to be made by professional searches that do not use difference imaging (e.g. MASTER, *Gaia*, CRTS), a larger fraction of other professional discoveries were made by surveys that do use difference imaging in 2016 than in previous years due to the start of the ATLAS survey. ASAS-SN continues to find sources with smaller median offsets than its competitors despite this fact, implying that the avoidance of the central regions of galaxies is still fairly

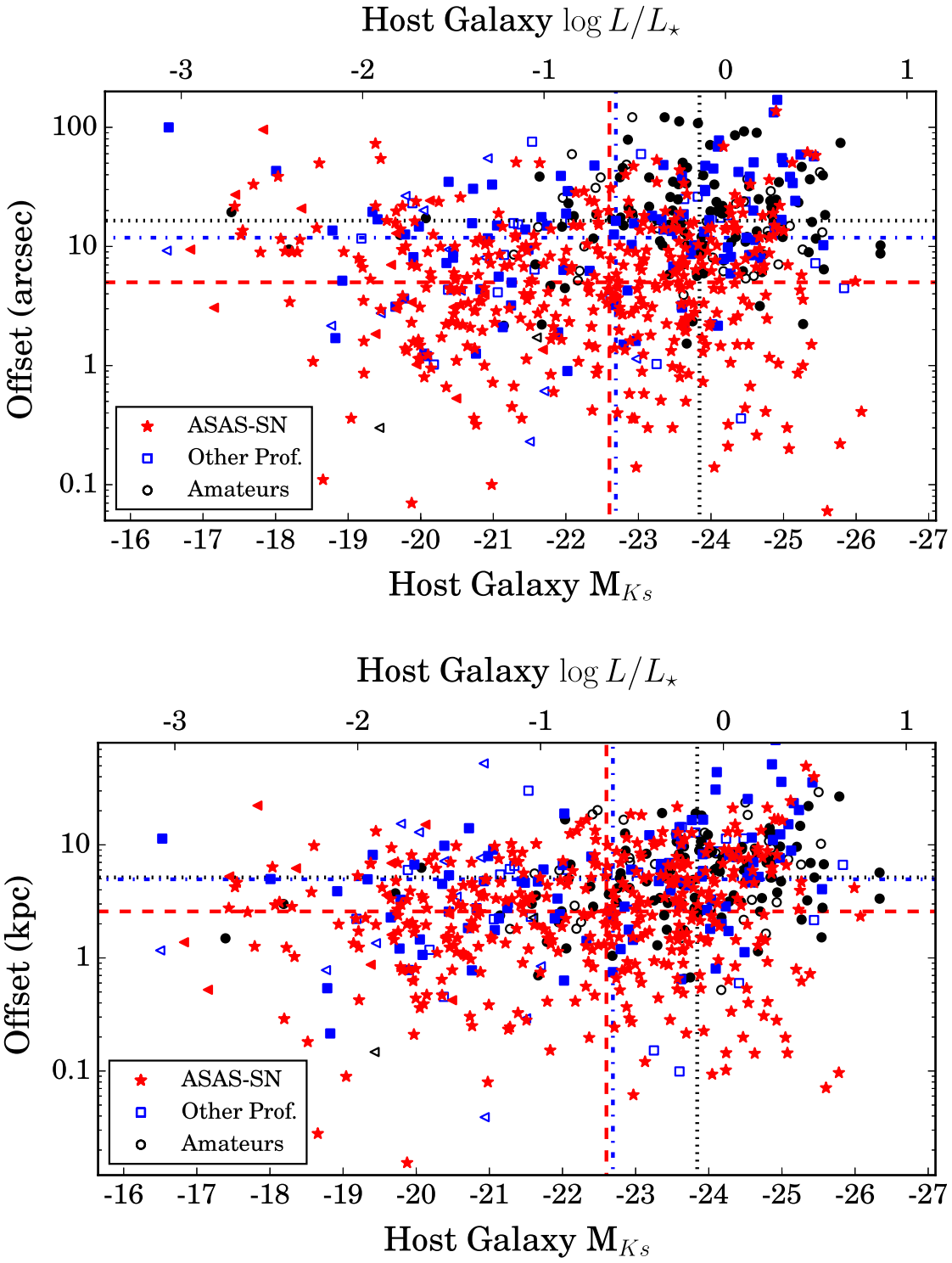

Figure 2. Upper panel: offset from the host nucleus in arcseconds compared to the absolute K_S-band host magnitude for all SNe in our combined sample discovered between 2014 May 1 and 2016 December 31. The top axis shows $\log(L/L_\star)$ values corresponding to the magnitude range shown on the bottom scale assuming $M_{\star,K_S} = -24.2$ (Kochanek et al. 2001). ASAS-SN supernova discoveries are shown as red stars, amateur discoveries are shown as black circles and discoveries by other professional searches are shown as blue squares. Triangles indicate upper limits on the host galaxy magnitudes for hosts that were not detected in 2MASS or *WISE*. Points are filled for SNe that were independently recovered by ASAS-SN. We indicate the median offsets and host magnitudes for ASAS-SN discoveries, amateur discoveries and other professional discoveries using dashed, dotted and dash–dotted lines, respectively, in colours that match the data points. Lower panel: as above, but with the offset measured in kiloparsecs.

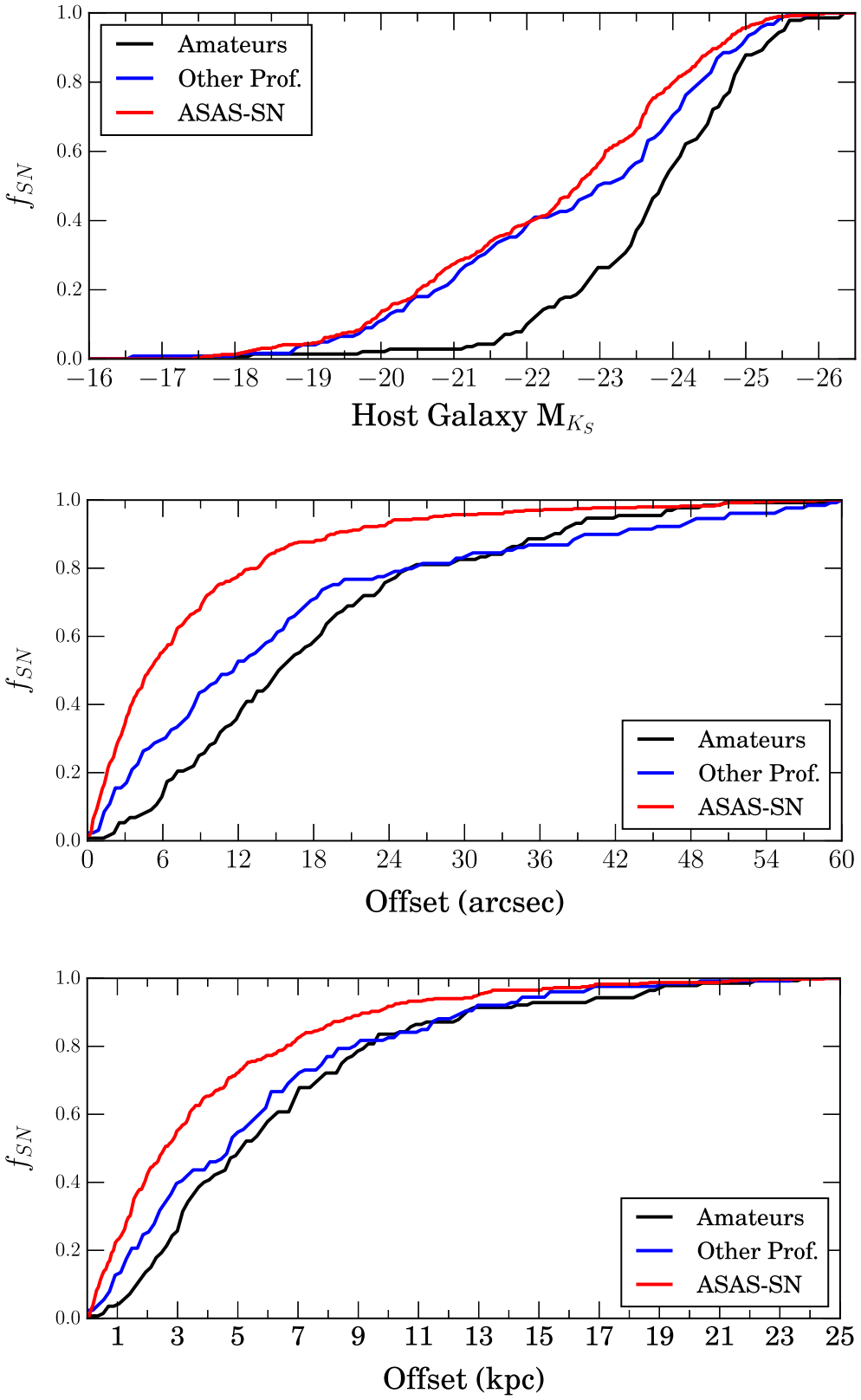

Figure 3. Cumulative, normalized distributions of host galaxy absolute magnitude (upper panel), offset from host nucleus in arcseconds (centre panel), and offset from host nucleus in kpc (bottom panel) for the ASAS-SN supernova sample (red), the other professional sample (blue) and the amateur sample (black). These figures further illustrate the trends from Fig. 2: amateur discoveries are clearly more biased towards more luminous hosts than professional surveys (including ASAS-SN), while ASAS-SN finds SNe at smaller offsets, regardless of whether offset is measured in arcseconds or kpc.

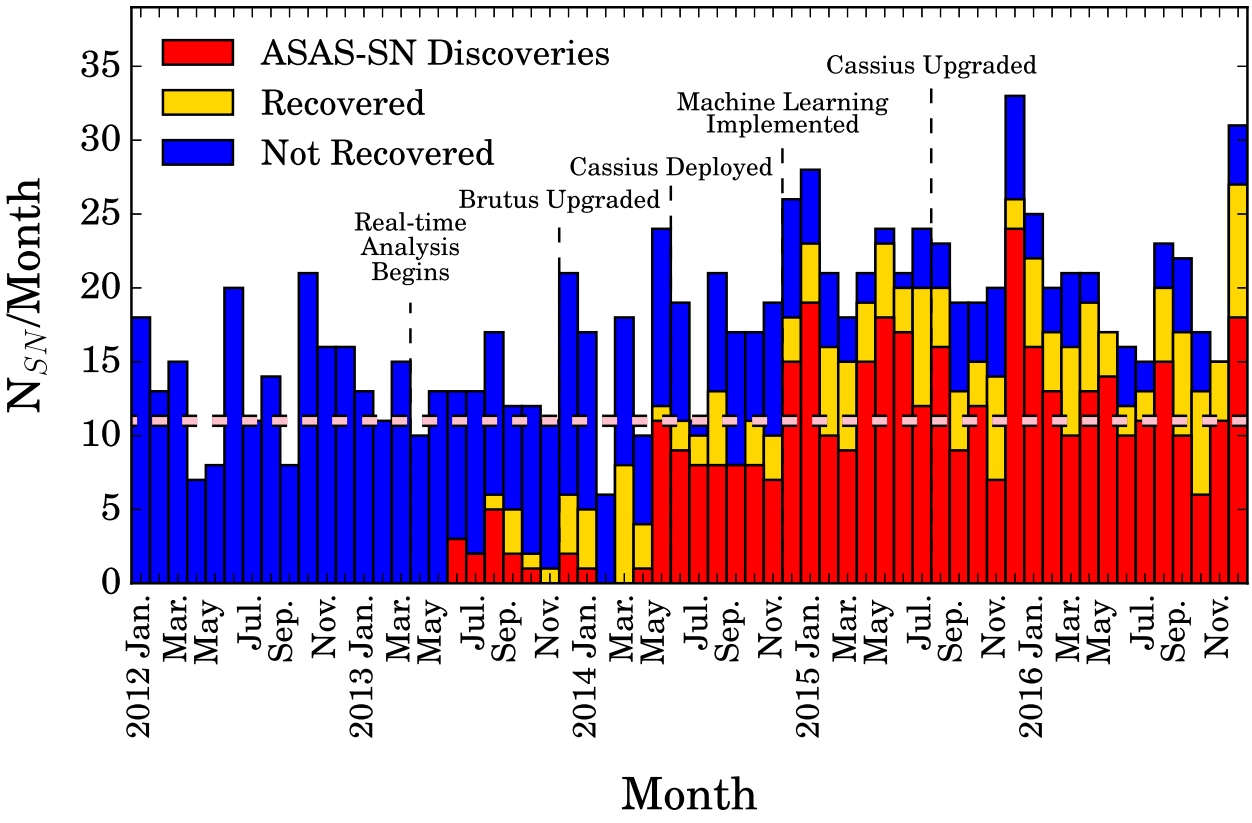

Figure 4. Histogram of bright SN discoveries in each month from 2012 through 2016. ASAS-SN discoveries are shown in red, SNe discovered by other sources and recovered in ASAS-SN data are shown in yellow and SNe that were not recovered by ASAS-SN are shown in blue. Significant milestones in the ASAS-SN timeline are also shown. The dashed pink line shows the median number of SNe discovered in each month from 2010 through 2012. The number of bright SN discoveries has exceeded this previous median in every month since ASAS-SN became operational in both hemispheres in 2014 May, and ASAS-SN discoveries account for at least half of all bright SN discoveries in every month since 2014 April.

common in surveys other than ASAS-SN, regardless of survey strategy and techniques.

The median host magnitudes are $M_{K_S} \simeq -22.6$, $M_{K_S} \simeq -22.8$ and $M_{K_S} \simeq -23.8$ for ASAS-SN discoveries, other professional discoveries and amateur discoveries, respectively. There remains a clear distinction between professional surveys (including ASAS-SN) and amateurs in terms of host luminosity, and ASAS-SN discoveries now have a fainter median than those of other professional surveys.

As we have shown previously, one way the impact of ASAS-SN on the discovery of bright SNe can be seen is by looking at the number of bright SNe discovered per month in recent years (e.g. Holoien et al. 2017a). In Fig. 4, we show the number of SNe with $m_{\rm peak} \leq 17$ per month in each month from 2012 through 2016. Milestones in the ASAS-SN timeline, such as the deployment of our southern unit Cassius and software improvements, are shown on the figure to help visualize the impact of these hardware and software improvements.

In its first year of operation, ASAS-SN had little effect on the number of bright SNe being discovered per month: the average number of bright SNe discovered per month from 2012 January through 2013 May was 13 with a scatter of 4 SNe per month, and from 2013 June through 2014 May the average was 15 with a scatter of 5 SNe per month. However, the addition of our southern unit Cassius and improvements to our pipeline dramatically impacted our detection efficiency and survey cadence, resulting in a significant increase in the number of SNe discovered per month: since ASAS-SN became operational in both hemispheres, the average number of bright SN discoveries has increased to 20 with a scatter of 5 SNe per month. This indicates that ASAS-SN has increased the rate of bright SNe discovered per month since becoming operational in the Southern hemisphere, from $\sim$13 $\pm$ 2 SNe per month to $\sim$20 $\pm$ 2 SNe per month, and has continued to maintain this increased rate for the last 2.5 yr – the addition of the 2016 SNe has only decreased the average number of discoveries by 1 SN per month from the previous 2014+2015 sample (Holoien et al. 2017a). ASAS-SN is discovering SNe that otherwise would not be found, allowing us to construct a more complete sample of bright, nearby SNe than was previously possible.

Fig. 5 shows the redshift distribution of our full sample, divided by type. There is a clear distinction between the three types shown, with the Type Ia distribution peaking between $z = 0.03$ and 0.035, the Type II distribution peaking between $z = 0.01$ and 0.015 and the Type Ib/Ic distribution peaking between $z = 0.015$ and 0.02. Type Ia SNe have a more luminous mean peak luminosity than core-collapse SNe, so this distribution is expected for our magnitude-limited sample, and is similar to what we have seen in our previous catalogs (Holoien et al. 2017a,b).

Finally, we show a cumulative histogram of SN peak magnitudes with $13.5 < m_{\rm peak} < 17.0$ in Fig. 6. As in our previous catalogues, the figure shows ASAS-SN discoveries, ASAS-SN discoveries and SNe recovered by ASAS-SN, and all SNe from our sample separately. While amateur observers still account for a large number of the brightest discoveries (those with $m_{\rm peak} \lesssim 14.5$; Holoien et al.

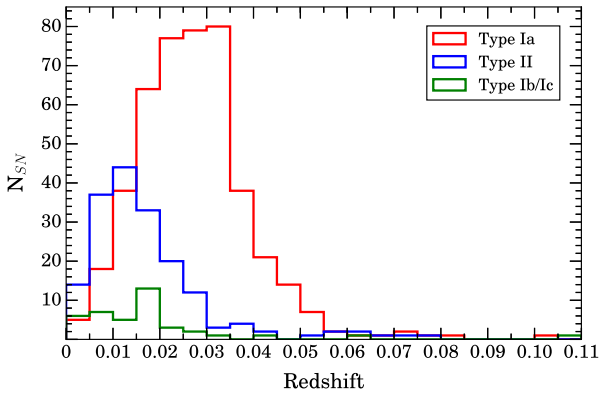

Figure 5. Histograms of SN redshifts from our complete sample with a bin width of $z = 0.005$. Distributions for Type Ia (red line), Type II (blue line) and Type Ib/Ic (green line) SNe are shown separately, with subtypes (such as SN 1991T-like and SN 1991bg-like Type Ia SNe) included as part of their parent groups. As expected due to their larger intrinsic brightness, Type Ia SNe are predominantly found at higher redshifts, while less luminous core-collapse SNe are found at comparatively lower redshifts.

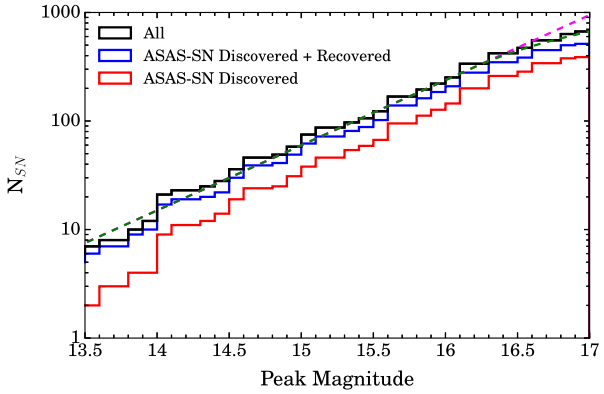

Figure 6. Cumulative histogram of SN peak magnitudes using a 0.1 mag bin width. The distributions for only ASAS-SN discoveries (red line), ASAS-SN discoveries and SNe recovered independently by ASAS-SN (blue line) and all SNe in the sample (black line) are shown separately. The green dashed line shows a broken power-law fit that has been normalized to the complete sample with a Euclidean slope below the break magnitude and a variable slope for fainter sources, and the lavender dashed line shows an extrapolation of the Euclidean slope to $m = 17$. The sample is roughly 70 per cent complete for $m_{\rm peak} < 17$.

2017a), ASAS-SN has discovered a significant fraction of these very bright SNe in 2015 and 2016, accounting for roughly half of such discoveries in our complete sample. ASAS-SN recovers the vast majority of such very bright cases that it does not discover, showing that it is competitive with amateurs who observe the small number of very low-redshift galaxies with high cadence. ASAS-SN discovered or recovered every SN with $m_{\rm peak} < 14.3$ in 2016 and accounts for a large fraction of the brightest SNe overall.

Fig. 6 also illustrates an estimate of the completeness of our sample. We fit a broken power law (shown with a green dashed line in the figure) to the magnitudes of the observable SNe brighter than $m_{\rm peak} = 17.01$, assuming a Euclidean slope below the break magnitude and a variable slope for higher magnitudes. We derived the parameters of the fit using Markov Chain Monte Carlo methods. For only the SNe discovered by ASAS-SN in our complete sample, the number counts are consistent with the Euclidean slope down to $m = 16.34 \pm 0.07$, similar to what we found in the 2015 sample (Holoien et al. 2017a). We find break magnitudes of $m = 16.26 \pm 0.06$ and 16.19 ± 0.09 for the sample of SNe discovered and recovered by ASAS-SN and the sample of all bright SNe, respectively, again similar to the 2015 results.

We find that the integral completenesses of the three samples relative to Euclidean predictions are 0.97 ± 0.02 (0.68 ± 0.03), 0.94 ± 0.02 (0.65 ± 0.03) and 0.93 ± 0.03 (0.71 ± 0.03) at 16.5 (17.0) mag for the ASAS-SN discovered sample, the ASAS-SN discovered + recovered sample and the total sample, respectively. The differential completenesses relative to Euclidean predictions are 0.71 ± 0.10 (0.22 ± 0.04), 0.62 ± 0.06 (0.22 ± 0.04) and 0.67 ± 0.05 (0.36 ± 0.04) at 16.5 (17.0) mag, respectively. These results imply that roughly 70 per cent of the SNe brighter than $m_{\rm peak} = 17$ are being found, and that 20–30 per cent of the $m_{\rm peak} = 17$ SNe are being found, relative to the Euclidean expectation extrapolated from brighter SNe, an improvement over the 15–20 per cent seen in the 2015 sample. The Euclidean approximation used here does not take into account deviations from Euclidean geometry, the effects of time dilation on SN rates, or *K*-corrections, and thus likely modestly underestimates the true completeness for faint SNe. These higher order corrections will be included when we carry out a full analysis of nearby SN rates.

4 CONCLUSIONS

This paper represents a comprehensive catalogue of spectroscopically confirmed bright SNe and their hosts from the ASAS-SN team, comprising 248 SNe discovered by ASAS-SN, other professional surveys, and amateur observers in 2016. Our total combined bright SN sample now includes 668 SNe, 387 discovered by ASAS-SN. The combined sample remains similar to that of an ideal magnitude-limited sample from Li et al. (2011) with a smaller proportion of Type Ia SN relative to core-collapse SNe than expected.

ASAS-SN is the only professional survey that provides a complete, rapid-cadence, all-sky survey of the nearby transient Universe, and continues to have a major impact on the discovery and follow-up of bright SNe. Even with the advent of recent professional surveys, amateur astronomers, who focus on bright and nearby galaxies for their SN searches, remain the primary competition to ASAS-SN for new discoveries. Our analyses show that ASAS-SN continues to find SNe that would not be found otherwise (e.g. Fig. 4) and that it finds SNe closer to galactic nuclei and in less luminous hosts than its competitors (Fig. 2). In 2016, ASAS-SN recovered the majority of bright SNe that it did not discover, as was the case in 2015, and discovered or recovered all but one of the very bright ($m_{\rm peak} \leq 15$) SNe that were discovered in 2016.

Our sample completeness is comparable to what it was at the end of 2015. Fig. 6 shows that the magnitude distribution of SNe discovered between 2014 May 1 and 2016 December 31 is roughly complete to a peak magnitude of $m_{\rm peak} = 16.2$, slightly worse than in 2015, but that it is roughly 70 per cent complete for $m_{\rm peak} \leq 17.0$, a slight improvement over 2015. This analysis serves as a precursor to rate calculations, which will be presented in Holoien et al. (in preparation). These rate calculations may have a significant impact on a number of fields, including the nearby core-collapse rate (e.g. Horiuchi et al. 2011, 2013) and multimessenger studies ranging from gravitational waves (e.g. Ando et al. 2013; Nakamura et al. 2016), to MeV gamma rays from Type Ia SNe (e.g. Horiuchi & Beacom 2010; Diehl et al. 2014; Churazov et al. 2015) to GeV–TeV gamma rays and neutrinos from rare types of core-collapse SNe (e.g. Ando & Beacom 2005; Murase et al. 2011;

Abbasi et al. 2012). Such joint measurements would be a great increase in the scientific reach of ASAS-SN discoveries.

This is the third of a yearly series of bright SN catalogues provided by the ASAS-SN team, and it is our hope that these catalogues will provide convenient and useful repositories of bright SNe and their host galaxies that can be used for new and interesting population studies. ASAS-SN continues to discover many of the best and brightest transients in the sky, and these catalogues are one way in which we can use our unbiased sample to impact SN research now and in the future.

ACKNOWLEDGEMENTS

We thank A. Piascik and I. Shivvers for providing redshift measurements.

We thank Las Cumbres Observatory and its staff for their continued support of ASAS-SN.

ASAS-SN is supported by the Gordon and Betty Moore Foundation through grant GBMF5490 to the Ohio State University and National Science Foundation (NSF) grant AST-1515927. Development of ASAS-SN has been supported by NSF grant AST-0908816, the Center for Cosmology and AstroParticle Physics at the Ohio State University, the Mt Cuba Astronomical Foundation, the Chinese Academy of Sciences South America Center for Astronomy (CASSACA) and by George Skestos.

TW-SH is supported by the Department of Energy Computational Science Graduate Fellowship, grant number DE-FG02-97ER25308. JSB, KZS and CSK are supported by NSF grant AST-1515927. KZS and CSK are also supported by NSF grant AST-1515876. BJS is supported by NASA through Hubble Fellowship grant HST-HF-51348.001 awarded by the Space Telescope Science Institute, which is operated by the Association of Universities for Research in Astronomy, Inc., for NASA, under contract NAS 5-26555. Support for JLP is in part provided by FONDECYT through the grant 1151445 and by the Ministry of Economy, Development, and Tourism's Millennium Science Initiative through grant IC120009, awarded to The Millennium Institute of Astrophysics, MAS. SD and PC are supported by 'the Strategic Priority Research Program–The Emergence of Cosmological Structures' of the Chinese Academy of Sciences (Grant No. XDB09000000). SD, SB and PC are also supported by Project 11573003 supported by NSFC. JFB is supported by NSF grant PHY-1404311. JS acknowledges support from the Packard Foundation. MDS is supported by generous grants provided by the Danish Agency for Science and Technology and Innovation realized through a Sapere Aude Level 2 grant and the Villum foundation. PRW acknowledges support from the US Department of Energy as part of the Laboratory Directed Research and Development programme at LANL.

This research uses data obtained through the Telescope Access Program (TAP), which has been funded by 'the Strategic Priority Research Program–The Emergence of Cosmological Structures' of the Chinese Academy of Sciences (Grant No.11 XDB09000000) and the Special Fund for Astronomy from the Ministry of Finance.

This research has made use of the XRT Data Analysis Software (XRTDAS) developed under the responsibility of the ASI Science Data Center (ASDC), Italy. At Penn State the NASA *Swift* programme is support through contract NAS5-00136.

This research was made possible through the use of the AAVSO Photometric All-Sky Survey (APASS), funded by the Robert Martin Ayers Sciences Fund.

This research has made use of data provided by ASTROMETRY.NET (Barron et al. 2008; Lang et al. 2010).

This paper uses data products produced by the OIR Telescope Data Center, supported by the Smithsonian Astrophysical Observatory.

Observations made with the NASA *Galaxy Evolution Explorer* were used in the analyses presented in this manuscript. Some of the data presented in this paper were obtained from the Mikulski Archive for Space Telescopes (MAST). STScI is operated by the Association of Universities for Research in Astronomy, Inc., under NASA contract NAS5-26555. Support for MAST for non-*HST* data is provided by the NASA Office of Space Science via grant NNX13AC07G and by other grants and contracts.

Funding for SDSS-III has been provided by the Alfred P. Sloan Foundation, the Participating Institutions, the National Science Foundation and the US Department of Energy Office of Science. The SDSS-III website is http://www.sdss3.org/.

This publication makes use of data products from the Two Micron All Sky Survey, which is a joint project of the University of Massachusetts and the Infrared Processing and Analysis Center/California Institute of Technology, funded by NASA and the National Science Foundation.

This publication makes use of data products from the *Wide-field Infrared Survey Explorer*, which is a joint project of the University of California, Los Angeles and the Jet Propulsion Laboratory/California Institute of Technology, funded by NASA.

This research is based in part on observations obtained at the Southern Astrophysical Research (SOAR) telescope, which is a joint project of the Ministério da Ciência, Tecnologia, e Inovação (MCTI) da República Federativa do Brasil, the US National Optical Astronomy Observatory (NOAO), the University of North Carolina at Chapel Hill (UNC) and Michigan State University (MSU).

This research has made use of the NASA/IPAC Extragalactic Database (NED), which is operated by the Jet Propulsion Laboratory, California Institute of Technology, under contract with NASA.

REFERENCES

Abbasi R. et al., 2012, A&A, 539, A60
Albareti F. D. et al., 2016, preprint (arXiv:1608.02013)
Ando S., Beacom J. F., 2005, Phys. Rev. Lett., 95, 061103
Ando S. et al., 2013, Rev. Mod. Phys., 85, 1401
Balam D. D., Graham M. L., 2016a, Astron. Telegram, 8788
Balam D. D., Graham M. L., 2016b, Astron. Telegram, 9016
Balam D. D., Graham M. L., 2016c, Astron. Telegram, 9047
Baltay C. et al., 2013, PASP, 125, 683
Barron J. T., Stumm C., Hogg D. W., Lang D., Roweis S., 2008, AJ, 135, 414
Bersier D., 2016a, Astron. Telegram, 9253
Bersier D., 2016b, Astron. Telegram, 9258
Bersier D., 2016c, Astron. Telegram, 9273
Bersier D. et al., 2016, Astron. Telegram, 9697
Blanchard P. K. et al., 2017, ApJ, 843, 106
Blondin S., Tonry J. L., 2007, ApJ, 666, 1024
Bock G. et al., 2016a, Astron. Telegram, 8566
Bock G. et al., 2016b, Astron. Telegram, 8915
Bock G. et al., 2016c, Astron. Telegram, 9091
Bock G. et al., 2016d, Astron. Telegram, 9668
Bose S., Thorstensen J., Klusmeyer J., Stanek K., Prieto J., Dong S., 2016, Astron. Telegram, 9405
Brimacombe J. et al., 2016a, Astron. Telegram, 8539
Brimacombe J. et al., 2016b, Astron. Telegram, 8542
Brimacombe J. et al., 2016c, Astron. Telegram, 8652
Brimacombe J. et al., 2016d, Astron. Telegram, 8685
Brimacombe J. et al., 2016e, Astron. Telegram, 8703
Brimacombe J. et al., 2016f, Astron. Telegram, 8712

Brimacombe J. et al., 2016g, Astron. Telegram, 8897
Brimacombe J. et al., 2016h, Astron. Telegram, 8898
Brimacombe J. et al., 2016i, Astron. Telegram, 8979
Brimacombe J. et al., 2016j, Astron. Telegram, 9005
Brimacombe J. et al., 2016k, Astron. Telegram, 9057
Brimacombe J. et al., 2016l, Astron. Telegram, 9058
Brimacombe J. et al., 2016m, Astron. Telegram, 9117
Brimacombe J. et al., 2016n, Astron. Telegram, 9123
Brimacombe J. et al., 2016o, Astron. Telegram, 9188
Brimacombe J. et al., 2016p, Astron. Telegram, 9199
Brimacombe J. et al., 2016q, Astron. Telegram, 9212
Brimacombe J. et al., 2016r, Astron. Telegram, 9262
Brimacombe J. et al., 2016s, Astron. Telegram, 9270
Brimacombe J. et al., 2016t, Astron. Telegram, 9305
Brimacombe J. et al., 2016u, Astron. Telegram, 9332
Brimacombe J. et al., 2016v, Astron. Telegram, 9338
Brimacombe J. et al., 2016w, Astron. Telegram, 9344
Brimacombe J. et al., 2016x, Astron. Telegram, 9430
Brimacombe J. et al., 2016y, Astron. Telegram, 9439
Brimacombe J. et al., 2016z, Astron. Telegram, 9457
Brimacombe J. et al., 2016aa, Astron. Telegram, 9474
Brimacombe J. et al., 2016ab, Astron. Telegram, 9560
Brimacombe J. et al., 2016ac, Astron. Telegram, 9714
Brimacombe J. et al., 2016ad, Astron. Telegram, 9724
Brimacombe J. et al., 2016ae, Astron. Telegram, 9727
Brimacombe J. et al., 2016af, Astron. Telegram, 9785
Brimacombe J. et al., 2016ag, Astron. Telegram, 9796
Brimacombe J. et al., 2016ah, Astron. Telegram, 9798
Brimacombe J. et al., 2016ai, Astron. Telegram, 9804
Brimacombe J. et al., 2016aj, Astron. Telegram, 9812
Brimacombe J. et al., 2016ak, Astron. Telegram, 9822
Brimacombe J. et al., 2016al, Astron. Telegram, 9893
Brimacombe J. et al., 2017, Astron. Telegram, 9927
Brown T. M. et al., 2013, PASP, 125, 1031
Brown J. S., Shappee B. J., Holoien T. W.-S., Stanek K. Z., Kochanek C. S., Prieto J. L., 2016a, MNRAS, 462, 3993
Brown J. S. et al., 2016b, Astron. Telegram, 8496
Brown J. S. et al., 2016c, Astron. Telegram, 8537
Brown J. S. et al., 2016d, Astron. Telegram, 8647
Brown J. S. et al., 2016e, Astron. Telegram, 8736
Brown J. S. et al., 2016f, Astron. Telegram, 8775
Brown J. S. et al., 2016g, Astron. Telegram, 8885
Brown J. S. et al., 2016h, Astron. Telegram, 8930
Brown J. S. et al., 2016i, Astron. Telegram, 8947
Brown J. S. et al., 2016j, Astron. Telegram, 9001
Brown J. S. et al., 2016k, Astron. Telegram, 9127
Brown J. S. et al., 2016l, Astron. Telegram, 9222
Brown J. S. et al., 2016m, Astron. Telegram, 9227
Brown J. S. et al., 2016n, Astron. Telegram, 9278
Brown J. S. et al., 2016o, Astron. Telegram, 9341
Brown J. S. et al., 2016p, Astron. Telegram, 9354
Brown J. S. et al., 2016q, Astron. Telegram, 9395
Brown J. S. et al., 2016r, Astron. Telegram, 9445
Brown J. S. et al., 2016s, Astron. Telegram, 9484
Brown J. S. et al., 2016t, Astron. Telegram, 9494
Brown J. S. et al., 2016u, Astron. Telegram, 9571
Brown J. S. et al., 2016v, Astron. Telegram, 9584
Brown J. S. et al., 2016w, Astron. Telegram, 9601
Brown J. S. et al., 2016x, Astron. Telegram, 9602
Brown J. S. et al., 2016y, Astron. Telegram, 9666
Brown J. S. et al., 2016z, Astron. Telegram, 9898
Brown J. S., Holoien T. W.-S., Auchettl K., Stanek K. Z., Kochanek C. S., Shappee B. J., Prieto J. L., Grupe D., 2017, MNRAS, 466, 4904
Chambers K. C. et al., 2016, preprint (arXiv:1612.05560)
Chen P. et al., 2016a, Astron. Telegram, 9398
Chen P. et al., 2016b, Astron. Telegram, 9407
Chornock R. et al., 2016, Astron. Telegram, 8765
Churazov E. et al., 2015, ApJ, 812, 62
Cikota A. et al., 2016a, Astron. Telegram, 8613
Cikota A. et al., 2016b, Astron. Telegram, 9878
Cikota A. et al., 2016c, Astron. Telegram, 9889
Cruz I. et al., 2016a, Astron. Telegram, 8666
Cruz I. et al., 2016b, Astron. Telegram, 8784
Cruz I. et al., 2016c, Astron. Telegram, 8944
Cruz I. et al., 2016d, Astron. Telegram, 8953
Cruz I. et al., 2016e, Astron. Telegram, 9073
Diehl R. et al., 2014, Science, 345, 1162
Dimitriadis G. et al., 2016, Astron. Telegram, 8555
Dong S. et al., 2016a, Science, 351, 257
Dong S. et al., 2016b, Astron. Telegram, 8521
Dong S. et al., 2016c, Astron. Telegram, 8892
Dong S. et al., 2016d, Astron. Telegram, 9843
Drake A. J. et al., 2009, ApJ, 696, 870
Elias-Rosa N. et al., 2016a, Astron. Telegram, 8727
Elias-Rosa N. et al., 2016b, Astron. Telegram, 9090
Falco E., Macri L., Stringer K., Prieto J. L., Challis P., Kirshner R., 2016a, Astron. Telegram, 8636
Falco E., Challis P., Kirshner R., Berlind P., Calkins M., Prieto J. L., Stanek K. Z., 2016b, Astron. Telegram, 8896
Falco E., Calkins M., Challis P., Kirshner R., Prieto J. L., Stanek K. Z., 2016c, Astron. Telegram, 9118
Falco E., Calkins M., Challis P., Kirshner R., Prieto J. L., Stanek K. Z., 2016d, Astron. Telegram, 9219
Falco E., Calkins M., Challis P., Kirshner R., Prieto J. L., Stanek K. Z., 2016e, Astron. Telegram, 9237
Faran T. et al., 2016, Astron. Telegram, 8724
Fausnaugh M. et al., 2016, Astron. Telegram, 9146
Fernandez J. M. et al., 2016a, Astron. Telegram, 8628
Fernandez J. M. et al., 2016b, Astron. Telegram, 8796
Frank S., Prieto J. L., Stanek K. Z., 2016, Astron. Telegram, 8830
Fraser M. et al., 2016, Astron. Telegram, 9208
Frieman J. A. et al., 2008, AJ, 135, 338
Gal-Yam A., Mazzali P. A., Manulis I., Bishop D., 2013, PASP, 125, 749
Gall C. et al., 2016, Astron. Telegram, 9368
Godoy-Rivera D. et al., 2017, MNRAS, 466, 1428
Gorbovskoy E. S. et al., 2013, Astron. Rep., 57, 233
Harmanen J. et al., 2016, Astron. Telegram, 9326
Harutyunyan A. H. et al., 2008, A&A, 488, 383
Herczeg G. J. et al., 2016, ApJ, 831, 133
Hodgkin S. T., Wyrzykowski L., Blagorodnova N., Koposov S., 2013, Phil. Trans. R. Soc. A, 371, 20120239
Holoien T. W.-S. et al., 2014a, MNRAS, 445, 3263
Holoien T. W.-S. et al., 2014b, ApJ, 785, L35
Holoien T. W.-S. et al., 2016a, Acta Astron., 66, 219
Holoien T. W.-S. et al., 2016b, MNRAS, 455, 2918
Holoien T. W.-S. et al., 2016c, MNRAS, 463, 3813
Holoien T. W.-S. et al., 2016d, Astron. Telegram, 8569
Holoien T. W.-S. et al., 2016e, Astron. Telegram, 8614
Holoien T. W.-S., Godoy-Rivera D., Prieto J. L., 2016f, Astron. Telegram, 8955
Holoien T. W.-S. et al., 2016g, Astron. Telegram, 9011
Holoien T. W.-S. et al., 2016h, Astron. Telegram, 9086
Holoien T. W.-S. et al., 2016i, Astron. Telegram, 9195
Holoien T. W.-S. et al., 2016j, Astron. Telegram, 9336
Holoien T. W.-S. et al., 2016k, Astron. Telegram, 9555
Holoien T. W.-S. et al., 2016l, Astron. Telegram, 9568
Holoien T. W.-S. et al., 2016m, Astron. Telegram, 9825
Holoien T. W.-S. et al., 2016n, Astron. Telegram, 9838
Holoien T. W.-S. et al., 2017a, MNRAS, 467, 1098
Holoien T. W.-S. et al., 2017b, MNRAS, 464, 2672
Horiuchi S., Beacom J. F., 2010, ApJ, 723, 329
Horiuchi S., Beacom J. F., Kochanek C. S., Prieto J. L., Stanek K. Z., Thompson T. A., 2011, ApJ, 738, 154
Horiuchi S., Beacom J. F., Bothwell M. S., Thompson T. A., 2013, ApJ, 769, 113
Hosseinzadeh G., Arcavi I., McCully C., Howell D. A., Sand D., Valenti S., 2016a, Astron. Telegram, 8567

Hosseinzadeh G., Yang Y., Arcavi I., Howell D. A., McCully C., Valenti S., 2016b, Astron. Telegram, 8623
Hosseinzadeh G., Yang Y., Valenti S., Arcavi I., Howell D. A., McCully C., 2016c, Astron. Telegram, 8679
Hosseinzadeh G., Yang Y., McCully C., Arcavi I., Howell D. A., Valenti S., 2016d, Astron. Telegram, 8748
Hosseinzadeh G., Arcavi I., Yang Y., Howell D. A., Valenti S., McCully C., 2016e, Astron. Telegram, 8807
Hosseinzadeh G., Arcavi I., Howell D. A., McCully C., Valenti S., 2016f, Astron. Telegram, 9065
Hosseinzadeh G., Arcavi I., Howell D. A., McCully C., Valenti S., 2016g, Astron. Telegram, 9589
Hosseinzadeh G., Arcavi I., Howell D. A., McCully C., Valenti S., 2016h, Astron. Telegram, 9698
James P. et al., 2016, Astron. Telegram, 9581
Kaiser N. et al., 2002, in Tyson J. A., Wolff S., eds, Proc. SPIE Conf. Ser. Vol. 4836, Survey and Other Telescope Technologies and Discoveries. SPIE, Bellingham, p. 154
Kangas T. et al., 2016a, Astron. Telegram, 9060
Kangas T. et al., 2016b, Astron. Telegram, 9836
Kato T. et al., 2014a, PASJ, 66, 30
Kato T. et al., 2014b, PASJ, 66, 90
Kato T. et al., 2015, PASJ, 67, 105
Kato T. et al., 2016, PASJ, 68, 65
Kilpatrick C. D., Siebert M. R., Foley R. J., Pan Y.-C., Jha S. W., Rest A., Scolnic D., 2016a, Astron. Telegram, 9361
Kilpatrick C. D., Siebert M. R., Coulter D. A., Foley R. J., Pan Y.-C., Jha S. W., Rest A., Scolnic D., 2016b, Astron. Telegram, 9367
Kiyota S. et al., 2016a, Astron. Telegram, 8549
Kiyota S. et al., 2016b, Astron. Telegram, 8607
Kiyota S. et al., 2016c, Astron. Telegram, 8621
Kiyota S. et al., 2016d, Astron. Telegram, 8882
Kiyota S. et al., 2016e, Astron. Telegram, 8939
Kiyota S. et al., 2016f, Astron. Telegram, 9020
Kiyota S. et al., 2016g, Astron. Telegram, 9045
Kiyota S. et al., 2016h, Astron. Telegram, 9815
Kochanek C. S. et al., 2001, ApJ, 560, 566
Koff R. A. et al., 2016a, Astron. Telegram, 8609
Koff R. A. et al., 2016b, Astron. Telegram, 9194
Lang D., Hogg D. W., Mierle K., Blanton M., Roweis S., 2010, AJ, 139, 1782
Law N. M. et al., 2009, PASP, 121, 1395
Leloudas G. et al., 2016, Nature Astron., 1, 0002
Li W. D. et al., 2000, in Holt S. S., Zhang W. W., eds, AIP Conf. Proc. Vol. 522, Cosmic Explosions: Tenth Astrophysics Conference. Am. Inst. Phys., New York, p. 103
Li W. et al., 2011, MNRAS, 412, 1441
Magee M. et al., 2016, Astron. Telegram, 8902
Marples P. et al., 2016a, Astron. Telegram, 9393
Marples P. et al., 2016b, Astron. Telegram, 9880
Marples P. et al., 2016c, Astron. Telegram, 9914
Masi G. et al., 2016a, Astron. Telegram, 8556
Masi G. et al., 2016b, Astron. Telegram, 8565
Masi G. et al., 2016c, Astron. Telegram, 8594
Masi G. et al., 2016d, Astron. Telegram, 8660
Masi G. et al., 2016e, Astron. Telegram, 8801
Masi G. et al., 2016f, Astron. Telegram, 9114
Masi G. et al., 2016g, Astron. Telegram, 9217
Masi G. et al., 2016h, Astron. Telegram, 9223
Masi G. et al., 2016i, Astron. Telegram, 9918
Mattila S. et al., 2016, Astron. Telegram, 8992
Monard L. A. G. et al., 2016a, Astron. Telegram, 8776
Monard L. A. G. et al., 2016b, Astron. Telegram, 9059
Morrell N., Shappee B. J., 2016a, Astron. Telegram, 9170
Morrell N., Shappee B. J., 2016b, Astron. Telegram, 9300
Morrell N., Phillips M., Bose S., Dong S., Shappee B. J., 2016a, Astron. Telegram, 9899
Morrell N., Phillips M., Shappee B. J., Dong S., 2016b, Astron. Telegram, 9900
Morrissey P. et al., 2007, ApJS, 173, 682
Murase K., Thompson T. A., Lacki B. C., Beacom J. F., 2011, Phys. Rev. D, 84, 043003
Nakamura K., Horiuchi S., Tanaka M., Hayama K., Takiwaki T., Kotake K., 2016, MNRAS, 461, 3296
Nicholls B. et al., 2016a, Astron. Telegram, 9079
Nicholls B. et al., 2016b, Astron. Telegram, 9081
Nicholls B. et al., 2016c, Astron. Telegram, 9671
Nicholls B. et al., 2016d, Astron. Telegram, 9713
Nicholls B. et al., 2016e, Astron. Telegram, 9826
Nicholls B. et al., 2016f, Astron. Telegram, 9827
Nicolas J. et al., 2016a, Astron. Telegram, 9254
Nicolas J. et al., 2016b, Astron. Telegram, 9349
Nicolas J. et al., 2016c, Astron. Telegram, 9422
Nicolas J. et al., 2016d, Astron. Telegram, 9611
Nielsen M. et al., 2016, Astron. Telegram, 9630
Pan Y.-C., Downing S., Foley R. J., Jha S. W., Rest A., Scolnic D., 2016a, Astron. Telegram, 8506
Pan Y.-C., Kilpatrick C. D., Siebert M. R., Foley R. J., Jha S. W., Rest A., Scolnic D., 2016b, Astron. Telegram, 9333
Pan Y.-C., Duarte A. S., Foley R. J., Jha S. W., Rest A., Scolnic D., 2016c, Astron. Telegram, 9696
Pan Y.-C., Foley R. J., Jha S. W., Rest A., Scolnic D., 2016d, Astron. Telegram, 9904
Piascik A. S., Steele I. A., 2016a, Astron. Telegram, 8505
Piascik A. S., Steele I. A., 2016b, Astron. Telegram, 8560
Piascik A. S., Steele I. A., 2016c, Astron. Telegram, 8634
Piascik A. S., Steele I. A., 2016d, Astron. Telegram, 8794
Piascik A. S., Steele I. A., 2016e, Astron. Telegram, 8798
Piascik A. S., Steele I. A., 2016f, Astron. Telegram, 9221
Pignata G. et al., 2009, in Giobbi G., Tornambe A., Raimondo G., Limongi M., Antonelli L. A., Menci N., Brocato E., eds, AIP Conf. Proc. Vol. 1111, Probing Stellar Populations Out to the Distant Universe: Cefalu 2008. Am. Inst. Phys., New York, p. 551
Post R. S. et al., 2016a, Astron. Telegram, 9837
Post R. S. et al., 2016b, Astron. Telegram, 9875
Prieto J. L., 2016, Astron. Telegram, 8867
Prieto J. L., Shappee B. J., 2016a, Astron. Telegram, 8924
Prieto J. L., Shappee B. J., 2016b, Astron. Telegram, 8936
Prieto J. L. et al., 2016a, ApJ, 830, L32
Prieto J. L., Rich J., Shappee B. J., 2016b, Astron. Telegram, 8629
Prieto J. L., Morrell N., Rudie G., Shappee B. J., 2016c, Astron. Telegram, 9142
Prieto J. L., Seibert M., Shappee B. J., Dong S., Stanek K. Z., 2016d, Astron. Telegram, 9701
Prieto J. L., Madore B. F., Shappee B. J., Seidel M. K., Dong S., Stanek K. Z., 2016e, Astron. Telegram, 9805
Prieto J. L., Seidel M. K., Shappee B. J., Stanek K. Z., 2017, Astron. Telegram, 9932
Pursiainen M. et al., 2016, Astron. Telegram, 9717
Quimby R. M., 2006, PhD thesis, Univ. Texas at Austin
Reynolds T. et al., 2016, Astron. Telegram, 9272
Romero-Cañizales C., Prieto J. L., Chen X., Kochanek C. S., Dong S., Holoien T. W.-S., Stanek K. Z., Liu F., 2016, ApJ, 832, L10
Rui L., Wang X., Huang F., Zhang T., Zhai M., 2016a, Astron. Telegram, 8532
Rui L., Wang X., Huang F., Zhai M., Zhang T., 2016b, Astron. Telegram, 8771
Schlafly E. F., Finkbeiner D. P., 2011, ApJ, 737, 103
Schmidt S. J. et al., 2014, ApJ, 781, L24
Schmidt S. J. et al., 2016, ApJ, 828, L22
Seidel M. K., Seibert M., Morrell N., Shappee B. J., 2016, Astron. Telegram, 9916
Seidel M. K., Morrell N., Shappee B. J., 2017, Astron. Telegram, 9922

Shappee B. J. et al., 2014, ApJ, 788, 48
Shappee B. J. et al., 2016a, ApJ, 826, 144
Shappee B. J. et al., 2016b, Astron. Telegram, 8502
Shappee B. J. et al., 2016c, Astron. Telegram, 9268
Shappee B. J., Prieto J. L., Rich J., Seibert M., Madore B., Poetrodjojo H., D'Agostino J., 2016d, Astron. Telegram, 9409
Shappee B. J., Prieto J. L., Rich J., Madore B., Poetrodjojo H., D'Agostino J., 2016e, Astron. Telegram, 9461
Shields J. et al., 2016, Astron. Telegram, 9353
Short L. et al., 2016a, Astron. Telegram, 9483
Short L. et al., 2016b, Astron. Telegram, 9566
Skrutskie M. F. et al., 2006, AJ, 131, 1163
Smith K. W. et al., 2016, Astron. Telegram, 9886
Somero A. et al., 2016, Astron. Telegram, 9734
Stone G. et al., 2016, Astron. Telegram, 9887
Strader J., Prieto J. L., 2017, Astron. Telegram, 9940
Strader J., Chomiuk L., Shishkovsky L., 2016a, Astron. Telegram, 8880
Strader J. et al., 2016b, Astron. Telegram, 8965
Strader J., Chomiuk L., Prieto J. L., 2016c, Astron. Telegram, 9233
Strader J., Chomiuk L., Shishkovsky L., 2016d, Astron. Telegram, 9850
Strader J., Chomiuk L., Salinas R., 2016e, Astron. Telegram, 9897
Taubenberger S. et al., 2016, Astron. Telegram, 8708
Terndrup D. M., Calhoun G., Cannata R., Schulze J., Dong S., Prieto J. L., 2016, Astron. Telegram, 9075
Terreran G. et al., 2016a, Astron. Telegram, 8694
Terreran G. et al., 2016b, Astron. Telegram, 9417
Tomasella L. et al., 2016a, Astron. Telegram, 8672
Tomasella L. et al., 2016b, Astron. Telegram, 9024
Tomasella L., Benetti S., Cappellaro E., Elias-Rosa N., Ochner P., Pastorello A., Terreran G., Turatto M., 2016c, Astron. Telegram, 9420
Tomasella L. et al., 2016d, Astron. Telegram, 9610
Tonry J. L., 2011, PASP, 123, 58
Tonry J., Denneau L., Stalder B., Heinze A., Sherstyuk A., Rest A., Smith K. W., Smartt S. J., 2016, Astron. Telegram, 8680
Turatto M., Benetti S., Tomasella L., Cappellaro E., Elias-Rosa N., Ochner P., Terreran G., 2016, Astron. Telegram, 9829
Wiethoff W. et al., 2016, Astron. Telegram, 8763
Wright E. L. et al., 2010, AJ, 140, 1868
Wyrzykowski Ł. et al., 2014, Acta Astron., 64, 197
Xiang D., Rui L., Wang X., Yang Q., Wu X., Xiao F., Fan Z., Zhang T., 2017, Astron. Telegram, 9926
Xin Y.-X., Zhang J.-J., 2016, Astron. Telegram, 8540
Yamanaka M. et al., 2017, ApJ, 837, 1
Yaron O., Gal-Yam A., 2012, PASP, 124, 668
Zhang J.-J., 2016, Astron. Telegram, 8550
Zhang J., Zheng X., Wang X., Rui L., 2016, Astron. Telegram, 9093

SUPPORTING INFORMATION

Supplementary data are available at *MNRAS* online.

Table 1. ASAS-SN supernovae.
Table 2. Non-ASAS-SN supernovae.
Table 3. ASAS-SN supernova host galaxies.
Table 4. Non-ASAS-SN supernova host galaxies.

Please note: Oxford University Press is not responsible for the content or functionality of any supporting materials supplied by the authors. Any queries (other than missing material) should be directed to the corresponding author for the article.

[1]*Department of Astronomy, The Ohio State University, 140 West 18th Avenue, Columbus, OH 43210, USA*
[2]*Center for Cosmology and AstroParticle Physics (CCAPP), The Ohio State University, 191 W. Woodruff Ave, Columbus, OH 43210, USA*
[3]*Carnegie Observatories, 813 Santa Barbara Street, Pasadena, CA 91101, USA*
[4]*Núcleo de Astronomía de la Facultad de Ingeniería y Ciencias, Universidad Diego Portales, Av. Ejército 441, Santiago, Chile*
[5]*Millennium Institute of Astrophysics, Santiago,Chile*
[6]*Kavli Institute for Astronomy and Astrophysics, Peking University, Yi He Yuan Road 5, Hai Dian District, Beijing 100871, China*
[7]*Coral Towers Observatory, Cairns, QLD 4870, Australia*
[8]*Rochester Academy of Science, 1194 West Avenue, Hilton, NY 14468, USA*
[9]*Department of Physics, The Ohio State University, 191 W. Woodruff Ave, Columbus, OH 43210, USA*
[10]*Astrophysics Research Institute, Liverpool John Moores University, 146 Brownlow Hill, Liverpool L3 5RF, UK*
[11]*Department of Physics and Astronomy, Michigan State University, East Lansing, MI 48824, USA*
[12]*Harvard–Smithsonian Center for Astrophysics, 60 Garden St, Cambridge, MA 02138, USA*
[13]*Las Campanas Observatory, Carnegie Observatories, Casilla 601, La Serena,Chile*
[14]*Warsaw University Astronomical Observatory, Al. Ujazdowskie 4, PL-00-478 Warsaw, Poland*
[15]*Department of Physics and Astronomy, Aarhus University, Ny Munkegade 120, DK-8000 Aarhus C, Denmark*
[16]*Los Alamos National Laboratory, Mail Stop B244, Los Alamos, NM 87545, USA*
[17]*Runaway Bay Observatory, 1 Lee Road, Runaway Bay, QLD 4216, Australia*
[18]*DogsHeaven Observatory, SMPW Q25 CJ1 LT10B, Brasilia, DF 71745-501, Brazil*
[19]*Association Francaise des Observateurs d'Etoiles Variables (AFOEV), Observatoire de Strasbourg, 11 Rue de l'Universite, F-67000 Strasbourg, France*
[20]*Cruz Observatory, 1971 Haverton Drive, Reynoldsburg, OH 43068, USA*
[21]*Observatory Inmaculada del Molino, Hernando de Esturmio 46, Osuna, E-41640 Sevilla, Spain*
[22]*Variable Star Observers League in Japan, 7-1 Kitahatsutomi, Kamagaya, Chiba 273-0126, Japan*
[23]*Antelope Hills Observatory, 980 Antelope Drive West, Bennett, CO 80102, USA*
[24]*Roof Observatory Kaufering, Lessingstr. 16, D-86916 Kaufering, Germany*
[25]*Leyburn and Loganholme Observatories, 45 Kiewa Drive, Loganholme, QLD 4129, Australia*
[26]*Virtual Telescope Project, Via Madonna de Loco, I-47-03023 Ceccano (FR), Italy*
[27]*Kleinkaroo Observatory, Calitzdorp, St Helena 1B, PO Box 281, 6660 Calitzdorp, Western Cape, South Africa*
[28]*Mount Vernon Observatory, 6 Mount Vernon Place, Nelson, New Zealand*
[29]*Groupe SNAude France, 364 Chemin de Notre Dame, F-06220 Vallauris, France*
[30]*Post Observatory, Lexington, MA 02421, USA*
[31]*Sierra Remote Observatories, 44325 Alder Heights Road, Auberry, CA 93602, USA*
[32]*Department of Earth and Environmental Sciences, University of Minnesota, 230 Heller Hall, 1114 Kirby Drive, Duluth, MN 55812, USA*

This paper has been typeset from a TEX/LATEX file prepared by the author.